RSC Advances

ROYAL SOCIETY OF CHEMISTRY

www.rsc.org/advances

Effect of different Metal Oxides on the Catalytic Activity of γ-Al_2O_3-MgO Supported Bifunctional Heterogeneous Catalyst in Biodiesel Production from WCO

Muhammad Farooq[a,*], Anita Ramli[b],

[a]*Department of Fundamental and Applied Sciences, Universiti Teknologi PETRONAS (UTP) 31750 Tronoh, Perak, Malaysia*

[b]*Department of Fundamental and Applied Sciences, Universiti Teknologi PETRONAS (UTP) 31750 Tronoh, Perak, Malaysia*

Corresponding author: farooq_khann@yahoo.com

Abstract

The catalytic activity of different γ-Al_2O_3-MgO supported bifunctional solid catalysts was successfully evaluated by carrying simultaneous esterification-transesterification in waste cooking oil. The physicochemical properties of the synthesized catalysts were studied using different characterization techniques to identify a catalyst of proper configuration for proper operation conditions to develop sustainable and economical biodiesel production process. The results indicated that Mo-Mn/γ-Al_2O_3-15wt% MgO catalyst showed excellent performance in biodiesel production from selected waste cooking oil as compared with Mo-Zn/γ-Al_2O_3-15wt% MgO or Mo-Sn/γ-Al_2O_3-15wt% MgO catalysts and provided biodiesel yield of 91.4%. under optimal reaction conditions i.e. methanol/oil molar ratio of 27:1, 5 wt.% of catalyst amount and a reaction temperature of 100 °C for 4 h. The good catalytic activity could be attributed to the existence of optimal number of catalytically active sites on the surface of catalyst. Moreover, the catalyst showed substantial reusability in the biodiesel production from waste cooking oil.

* Corresponding author. Tel: +60-3990450
E-mail address: Farooq_khann@yahoo.com

1. Introduction.

The rapid dwindling of the fossil fuels and their associated environmental problems are top priority issues for both developed and developing nations of the world. Currently, fossil fuels provide approximately 87% of the total world energy demand, and are still the main source of the global energy demand and supply scenario[1]. It has been reported that under a business-as-usual scenario the reserves will last for 218 years for coal, 41 years for oil, and 63 years for natural gas[2, 3]. The world energy demand has increased dramatically over the last few decades due to fast advancement in huge industries and rapid growth in world's population. According to the EIA (2006d) report, it is estimated that the world's total energy consumption will be increased by the 59% between 1999 and 2020. Similarly, carbon dioxide, which is considered to be a primary greenhouse gas, emission will increased by 60% [4].

Therefore, it is essential to search for sustainable fuels so as to meet the world increasing energy demand, and which are environmentally more acceptable and efficient. Among alternative sources of fuel, biodiesel has attracted enormous interest due to its desired fuel properties such as less toxic, low cost, clean, high lubricating properties, lack of sulphur, less polluting fuel and not harmful to the environment[5, 6]. Various methods have been employed in biodiesel production such as blending, pyrolysis, micro emulsion , and transesterification[6]. However, transesterification is preferred because it shows high conversion of edible, non edible oil to biodiesel, give low viscosity biodiesel and the byproducts such as glycerin produced in transesterification reaction is commonly used for medicinal application[7]. Chemically, biodiesel is a long chain of fatty acid alkyl esters produced as a result of transesterification reaction from edible, non edible seed oil, waste cooking oil and animal fats. Transesterification is a process in

which triglyceride such as vegetable oil and animal fat react with alcohol in the presence of suitable catalyst to produce fatty acid methyl ester (FAME) [8].

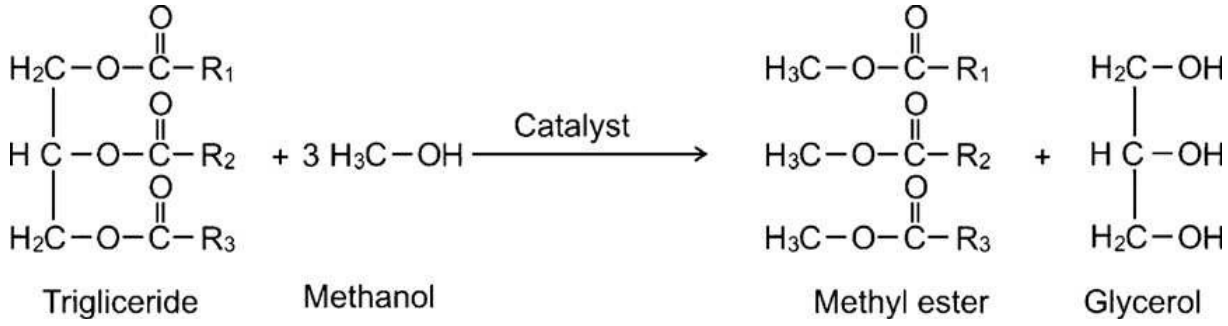

Figure .1 Transesterification of triglycerides in the presence of alcohol.

Currently, biodiesel production process is suffering from different technological challenges, such as highly effective catalysts to make the biodiesel production feasible for sustainable development. Homogeneous catalysts (base/acid) are commonly used for biodiesel production from different feedstocks under mild reaction conditions. However, these traditional catalysts cause several technical problems i.e. reaction corrosion, large amounts of waste water production, separation problems, thereby increase the cost of biodiesel production[9].

Heterogeneous catalysts are encouraged in biodiesel production instead of homogeneous catalysts due to their environmentally friendly behavior, reusability, carrying simple purification process, thereby resolve many of these problems associated with homogeneous catalyzed biodiesel technology[10].

Recently, among different heterogeneous catalysts, bifunctional acid-base solid catalysts have received a considerable attention in biodiesel production technology due to their environmental compatibility, high selectivity, thermal stability and reusability [11]. Bifunctional heterogeneous catalysts has the potential to carry efficiently simultaneous

esterification/transesterification reactions of the fatty acids and triglyceride present in the feedstocks, minimizing oil and biodiesel hydrolysis to avoid problems related with water and free fatty acid [12].

Similarly, feedstock is a principal parameter in biodiesel production technology. It has been reported that 70-95% of the total biodiesel production cost arises from the cost of feedstock (vegetable oil, animal fats)[13, 14]. Therefore, it is vital to select a suitable feedstock for economical and low cost biodiesel production. Large amounts of waste cooking oils and animal fats (millions of tons of WCO per day) are produced throughout the world, especially in the developed countries[15, 16]. Therefore, the management of such oils and fats has become a significant challenge due to their serious environmental hazards. In this context, the utilization of waste cooking for biodiesel production will not only provide economic and environmental benefits, but will also improve the efficiency in the use of waste materials. Additionally, the use of WCO for biodiesel production will surely avoid the competition with the same edible oil resources.

In the present studies, bifunctional heterogeneous catalysts have been synthesized and employed in biodiesel production from waste cooking oil for efficient and sustainable biodiesel technology. The physicochemical properties of the synthesized catalyst have been studied in detail to correlate them with the catalytic activity in order to design a catalyst of proper configuration with proper operating conditions for efficient and eco-friendly biodiesel production process.

2. Experimental

2.1. Catalyst preparation

Bifunctional heterogeneous catalysts supported on γ-Al_2O_3–MgO mixed oxides were prepared by modified wet impregnation method as reported in our previous studies[11]. γ-Al_2O_3–MgO mixed

oxide with different MgO loadings (5, 10, 15 and 20 wt% with respect to γ-Al_2O_3) were prepared by using simple impregnation method [17]. The γ-Al_2O_3–MgO supports were then impregnated with an aqueous solution of $(NH_4)_6Mo_7O_{24}\cdot 4H_2O$ with constant stirring to achieve 5 wt% Mo loading. During impregnation, a few drops of 0.01 M HNO_3 aqueous solution were added to attain the maximum adsorption of ions on the support. At pH below the PZC value, the protonated hydroxyl groups on the surface of the support increase i.e. the concentration of the adsorption sites for negative species ($M\text{-}OH_2^+$) increases and hence the adsorption of $Mo_7O_{24}^{6-}$ ions is favored as shown below.

$$M\text{-}OH + H^+ \rightarrow M\text{-}OH_2^+ \xrightarrow{Mo_7O_{24}^{6-}} (M\text{-}OH_2)_6^+ \; Mo_7O_{24}^{6-} \qquad \text{[Eq. 1]}$$

The mixture was stirred for 3 h at room temperature followed by slow evaporation of water by heating at 70 °C. The catalysts were then dried at 110 °C for 12 h and finally calcined at 500 °C in the presence of air in a muffle furnace for 5 h. The Mo/γ-Al_2O_3–MgO bifunctional heterogeneous catalysts were further modified with 5 wt% Mn, Zn and Sn metal oxides using the wet impregnation method. The catalysts were impregnated with an aqueous solution of respective metal nitrate salt at room temperature. However, during the preparation of the Mo–M/γ-Al_2O_3–MgO bimetallic catalyst, the impregnation was carried out slightly in a basic medium using a 0.01 M KOH aqueous solution to achieve the maximum adsorption of Mn, Zn or Sn on the support surface At pH above the PZC, the surface hydroxyl groups deprotonated, hence adorption of positive species (Sn^{2+}, Zn^{2+} or Mn^{2+}) is favoured as shown below.

$$M\text{-}OH + OH^- \xrightarrow{M^{2+}} (M\text{-}O)_2^- \; M^{2+} + H_2O \qquad \text{[Eq. 2]}$$

The catalyst was dried and then calcined at 500 °C temperature as determined from the TGA analysis.

2.2 Feedstock characterization.

The WCO was collected from the Universiti Teknologi PETRONAS cafeteria. The selected WCO was first filtered and then washed several times with hot distilled water to remove salt and other soluble materials prior to the reaction studies. The washed WCO was then treated with silica gel and the mixture was stirred for 3 h to remove the water used during washing, followed by vacuum filtration .The so treated oil was then dried at 110 °C for 24 h in an oven and stored in an air tight bottle for further studies.

The key physical and chemical characteristics of the selected WCO were studied by following standard test methods (Table 1).

Table 1. Physicochemical properties of the selected WCO.

Property	Unit	Value
Acid value	mg KOH/g	3.27
Peroxide value	mEq kg^{-1}	9.21
Calorific value	J/g	38462
Kinematic viscosity at 40 ºC	cSt	41.17
Specific gravity at 30 ºC	------	0.903
Saponification value	mg KOH/g	186.12
Flash point	^{o}C	274
Moisture content	wt%	0.102
Mean molecular mass	g/mol	920.42

2.3 Catalytic Experiments

The catalytic activity of the synthesized bifunctional catalysts was evaluated in biodiesel production from waste cooking oil via simultaneous esterification and transesterification reactions in three necked glass reactor fitted with a reflux condenser and thermometer. After reaction completion, biodiesel was recovered and the percent biodiesel yield was calculated by using the following formula as reported elsewhere in literature[18]. The quantification of the glycerine, monoglycerides, diglycerides and triglycerides was done by GC-FID according to the EN 14105: 2003 method [19, 20]. Moreover, the fatty acid methyl esters (FAMEs) profile of the product (synthesized biodiesel) were determined by gas chromatography coupled with mass spectrometer (GC-MS).

$$Biodiesel\ \ yield\,(\%) = \frac{Weight\ \ of\ \ biodiesel}{Weight\ \ of\ \ oil} \times 100 \qquad \text{[Eq. 3]}$$

3. Results and Discussion

3.1. Catalyst Characterization

3.1.1 N_2 Adsorption-Desorption Analysis

The surface area, pore volume and mean pore diameter of synthesized catalysts are reported in Table 2. The results show that the surface area, pore volume and average pore diameter decrease slightly when the monometallic Mo/γ-Al_2O_3-15 wt% MgO catalyst was modified with different metal oxides such as Sn, Zn or Mn. The decrease in the surface area, pore volume and average pore diameter are due to the fact that addition of the second metal oxide species blocks some of the pores of the support during preparation. However, the decrease in the surface area is very small, suggesting that the active metal species are highly dispersed on the support surface.

According to the IUPAC classification, all catalysts exhibit type IV isotherms with a well developed type H2 hysteresis loops, indicating the characteristics of mesoporous materials [21, 22]. Moreover, the catalysts show pore size in the mesoporous region with unimodal curve.

Table 2. Specific surface area (S_A), pore volume (V_P), and average pore diameter (D_P) of the synthesized catalyst.

Catalyst	S_A (m^2/g)	Vp (cm^3/g)	D_P (Å)
Mo/γ-Al_2O_3-15 wt% MgO	140	0.149	58.95
Mo-Sn/γ-Al_2O_3-15 wt% MgO	136	0.145	55.98
Mo-Zn/γ-Al_2O_3-15 wt% MgO	137	0.146	56.78
Mo-Mn/γ-Al_2O_3-15 wt% MgO	139	0.148	57.91

3.1.2 X-ray Diffraction Analysis

The XRD patterns of γ-Al_2O_3-15 wt% MgO supported bifunctional catalysts are depicted in Figure 2. The XRD patterns of each catalyst show the characteristic peaks of γ-Al_2O_3 at 2θ = 32.62°, 37.53°, 45.58° and 67°, and MgO at 42.75° and 62.11° respectively. However, no characteristic peaks corresponding to the active metals were detected in the XRD patterns. This suggests that the active metal oxides particles are highly dispersed on the support surface as reported by the Borowiecki et al. [23]. The intensities of the peaks corresponding to γ-Al_2O_3 and MgO in the XRD patterns decrease slightly when the active metal (Mo) and promoters (Sn, Zn or Mn) were introduced into the catalyst supports. The decrease in the intensities may be attributed to the strong metal-support interaction and formation of complex oxides at a very low

concentration on the surface of the support during calcination. The absence of the diffraction peaks of molybdenum oxide and different promoters (Sn, Zn or Mn) oxides could be attributed to the formation of finely dispersed metal crystallite species on the surface of the catalyst support which are below the detection limits of the XRD model used in this work. Thus, the XRD results are in good consistent with the results reported by the Li et al. [24].

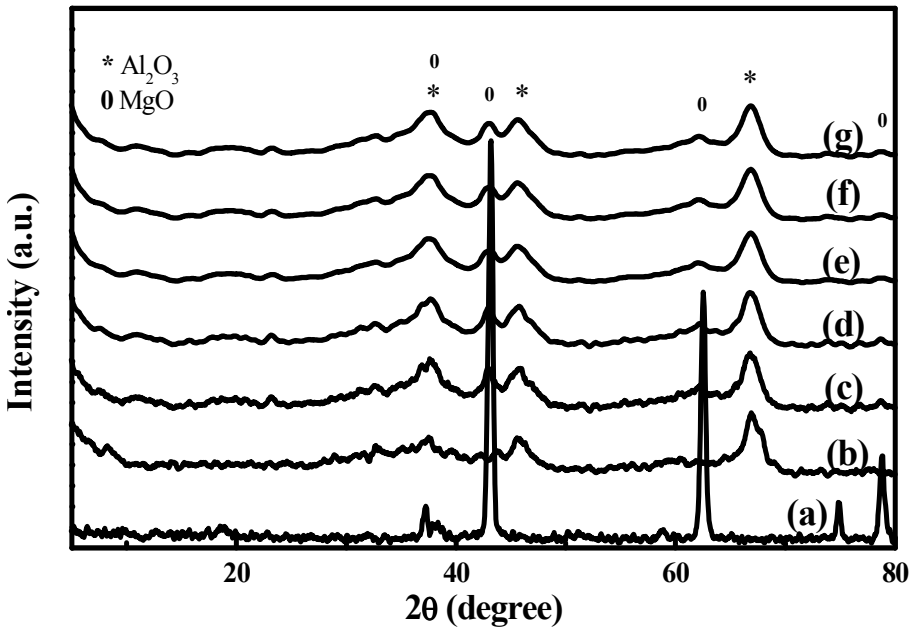

Figure 2. XRD patterns of (a) MgO (b) γ-Al_2O_3 (c) γ-Al_2O_3-15wt% MgO (d) Mo/γ-Al_2O_3-15wt% MgO (e) Mo-Sn/γ-Al_2O_3-15wt% MgO (f) Mo-Zn/γ-Al_2O_3-15wt% MgO (g) Mo-Mn/γ-Al_2O_3-15wt% MgO catalysts.

3.1.3 Temperature-Programmed Reduction Analysis

The states of different metals, interactions of metal oxide components among themselves and with the support were investigated by TPR analysis. The TPR profiles of γ-Al_2O_3-15 wt% MgO

supported catalysts are presented in Figure 3, and the data is further summarized in Table 3. The TPR profile of Mo/γ-Al_2O_3-15 wt% MgO catalyst is also shown for comparison. It can be seen from the TPR results that Mo-Sn/γ-Al_2O_3-15 wt% MgO catalyst displays two broad reduction peaks at 626 ^oC and 987 ^oC with a small shoulder peak at 708 ^oC. The first peak at 628 ^oC is attributed to the reduction of Mo^{6+} to Mo^{4+} species of polymeric Mo structures [25]. This reduction temperature is lower than that observed in the case of Mo/γ-Al_2O_3-15 wt% MgO, which indicates that the addition of Sn promoter decreases the molybdenum-support interaction, hence increases the reducibility of the catalyst. The reduction peak at 987 ^oC is attributed to the reduction of the metal species strongly bonded to the support and species produced during the reduction in the first stage, together with the partial reduction of the support [26]. The shoulder peak at 708 ^oC could be assigned to the reduction of some intermediate complex oxide species strongly bonded to support [27, 28]. However, these complex oxide species were not identified in the XRD results which indicate that these species are highly dispersed in the structure of catalyst.

Furthermore, there is no clear reduction peak which may be assigned to the reduction of Sn^{2+} to Sn^0. This may suggest that the reduction of Sn^{2+} occur in the same temperature region as the reduction of the Mo^{6+} to Mo^{4+} [29, 30].

On the other hand, Mo-Zn/γ-Al_2O_3-15 wt% MgO catalyst exhibits three reduction peaks at 533 ^oC, 608 ^oC and 982 ^oC with a shoulder peak of 717 ^oC. The peak at 533 ^oC is attributed to the reduction of the surface Mo^{6+} to Mo^{4+} species along with the reduction of the zinc oxide (Zn^{2+} to Zn^0) [31]. The peak appeared at 608 ^oC may be attributed to the further reduction of the Mo^{4+} species to the lower species (Mo^{2+}). The shoulder peak is attributed to the reduction of the intermediate metal oxide species. Similarly, the reduction peak appeared at 984 ^oC could be attributed to the metal species strongly bonded to support. The TPR profile shows that the

addition of Zn promoter into the Mo/γ-Al_2O_3-15 wt% MgO catalyst decreases the reduction temperature of Mo^{6+} to Mo^{4+} or lower species, indicating that Zn promotes the reducibility of the Mo^{6+} species in the bimetallic catalyst.

However, when Mn was incorporated into the Mo/γ-Al_2O_3-15 wt% MgO catalyst, the first reduction peak appeared at temperature as low as 343 ^oC which may be attributed to the reduction of manganese oxide from Mn^{2+} to Mn^0 and less stable metal species which are weakly bonded to the support [32]. The reduction peak appeared at 571 ^oC could be due to the reduction of the Mo species, whereas the shoulder peak at 703 ^oC could be due to the reduction of complex oxides present on the surface of the catalyst. Similarly, the reduction peak appeared at 1002 ^oC may be attributed to the reduction of highly stable species. Upon addition of Mn promoter, the reduction peak corresponding to reduction of Mo^{6+} to Mo^{4+} species is shifted to lower temperature, indicating weak metal-support interaction. This shows that Mn promoter enhanced the reducibility of the bimetallic catalyst. In addition, there is no clear reduction peak which may be assigned to the reduction of Mn^{2+} to Mn^0. This may suggest that the reduction of Mn^{2+} occur in the same temperature region as the reduction of the Mo^{6+} to Mo^{4+}.

In summary, when the TPR patterns of different bimetallic catalysts are compared, it is noted that the Zn modified catalyst shows enhanced reducibility as compared to other bimetallic catalysts prepared by the same method.

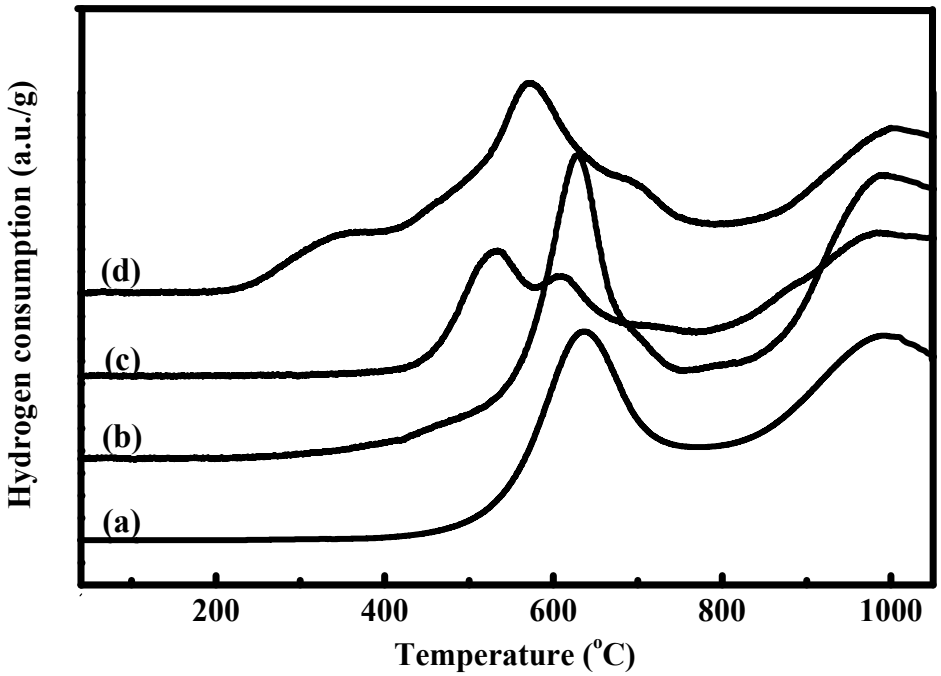

Figure 3. H_2-TPR profiles of (a) Mo/γ-Al_2O_3-15 wt% MgO (b) Mo-Sn/γ-Al_2O_3-15 wt% MgO (c) Mo-Zn/γ-Al_2O_3-15 wt% MgO (d) Mo-Mn/γ-Al_2O_3-15 wt% MgO catalysts.

Table 3. H_2-TPR data of different synthesized catalysts.

Catalyst	Reduction Temperature (°C)			
	Peak 1	Peak 2	Peak 3	Peak 4
Mo/γ-Al_2O_3-15 wt% MgO	642	995	/	/
Mo-Sn/γ-Al_2O_3-15 wt% MgO	626	708 (S)	987	/
Mo-Zn/γ-Al_2O_3-15 wt% MgO	533	608	717 (S)	982
Mo-Mn/γ-Al_2O_3-15 wt% MgO	343	571	703 (S)	1002

S = Shoulder peak

3.1.5 X-ray Photoelectron Spectroscopy Analysis

X-ray photoelectron spectroscopy was used to investigate the chemical environment of each element present on the surface of the γ-Al_2O_3-15 wt% MgO supported bimetallic catalysts. The representative XPS analysis results are shown in Figure 4, while the corresponding binding energies are listed in Table 4. Slight decrease in the binding energy of Mo 3d was observed when 5 wt% Sn, Zn or Mn were incorporated in the Mo/γ-Al_2O_3-15 wt% MgO catalyst. The difference in Mo 3d binding energy may be attributed to the changes in the elemental oxidation state and chemical environment, originated from different metal-support interaction. The decrease in the Mo 3d binding energy of bimetallic catalysts is attributed to the decrease in the metal-support interaction upon introduction of the second metal into the Mo/γ-Al_2O_3-15 wt% MgO catalyst as observed from the TPR results. The results further suggest that these promoters further prevent the formation of various types of spinels after calcination of the bimetallic catalyst [33]. Among different bimetallic catalysts, Mo-Zn/γ-Al_2O_3-15 wt% MgO catalyst exhibits lower Mo 3d binding energy, indicating comparatively weak metal-support interaction.

Miyoshi and Chung [34] suggested that the metal sites in the higher oxidation states would possess higher binding energies as compared with the metal sites in the lower oxidation states. The decrease in the Mo 3d binding energy of the γ-Al_2O_3-15 wt% MgO supported bimetallic catalyst could be attributed to the electron transfer from promoters to metallic Mo. As a result of electron transfer effect of promoters, the bimetallic catalysts attain an electron rich state, causing changes in the oxidation state [33]. Table 4 shows that the incorporation of Zn exhibits enhanced electron transfer ability. Thus, the XPS and TPR results are in good agreement which define the effect of promoters on the metal- support interaction and catalyst reducibility.

Similarly, the slight decrease in the binding energies of Al 2p and Mg 2p could be due to the

change in the chemical environment of Mg and Al upon addition of different promoters into the Mo/γ-Al_2O_3-15 wt% MgO catalyst. All the bimetallic catalysts contain 15 wt% MgO loading, which appeares as crystallites on the surface of all catalysts instead of monolayer formation. It has been reported that the binding energy of Mg 2p of dispersed phases (monolayer) of MgO is quite different from that of its crystalline species [35, 36].

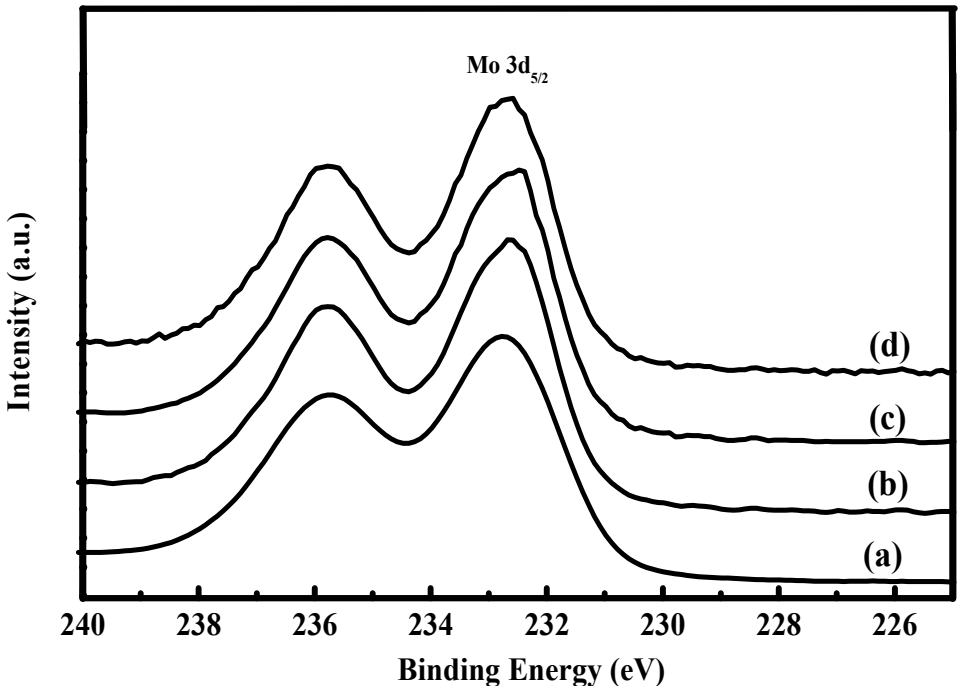

Figure 4. XPS spectra of Mo3d (a) Mo-Sn/γ-Al_2O_3-15 wt% MgO (b) Mo-Zn/γ-Al_2O_3-15 wt% MgO (c) Mo-Mn/γ-Al_2O_3-15 wt% MgO catalyst.

Table 4. Binding energies (eV) of different bifunctional catalysts obtained from XPS analysis.

Catalyst	Binding Energy (eV)					
	Al 2p	Mg 2p	Mo $3d_{5/2}$	Sn $3d_{5/2}$	Zn $2P_{3/2}$	Mn $2P_{3/2}$
Mo/γ-Al_2O_3-15 wt% MgO	74.37	49.55	232.75	----	----	-----
Mo-Sn/γ-Al_2O_3-15 wt% MgO	74.51	50.13	232.63	485.1	-----	-----
Mo-Zn/γ-Al_2O_3-15 wt% MgO	74.34	49.91	232.45	----	1020.51	-----
Mo-Mn/γ-Al_2O_3-15 wt% MgO	74.45	50.04	232.58	----	-----	642.64

3.1.6 Temperature Programmed Desorption of CO_2 and NH_3 Analysis

CO_2-TPD was performed to study the distribution of basic sites on the surface of the prepared catalysts. Generally, CO_2 adsorbed on the weaker basic sites is desorbed at low temperature and that adsorbed on the strong basic sites is desorbed at high temperature. The density of basic sites calculated from CO_2-TPD results are summarized in Table 5. The results demonstrate that Mo/γ-Al_2O_3 catalysts indicate the existence of only weak basic sites. However, the addition of MgO caused appearance of medium basic sites as well on the surface of bifunctional catalyst. The density of weak and medium basic sites further increased when Sn, Zn or Mn metal oxides are introduced into the catalyst. In addition, strong basic sites only appeared on the surface of catalyst in the case of Mn metal oxide. The strong basic sites are neutralized first when an acidic support is mixed chemically with the basic one, generating medium and weak basic sites in the MgO-γ-Al_2O_3 mixed oxides due to the redistribution [37]. This shows that the distribution of basic sites is influenced by the addition of MgO and active metals. Moreover, the presence of highly dispersed MgO and active metal species on the surface of γ-Al_2O_3 catalysts may influence the

strength of the basic sites [35]. The medium strength basic sites are related to the oxygen present in both Mg^{2+}–O^{2-} and Al^{3+}–O^{2-} pairs. The strong basic sites are related to the presence of O^{2-} ions associated with the cationic vacancies [38, 39]. The CO_2-TPD results of bimetallic catalysts further demonstrate that the amount of CO_2 uptake is higher for the Mo-Mn/γ-Al_2O_3-15 wt% MgO catalyst, showing greater number of basic sites on the surface of the catalyst. The co-existence of the basic sites of different strengths may play an important role to improve the catalytic activity in the biodiesel reactions.

Table 5. Density of basic sites of the prepared catalysts.

Catalyst	Density of basic sites (mmol/g)		
	Weak	Medium	Strong
Mo/γ-Al_2O_3	0.64	n.d.	n.d.
Mo/γ-Al_2O_3-15 wt% MgO	0.11	0.46	n.d
Mo-Sn/γ-Al_2O_3-15 wt% MgO	0.98	0.52	n.d.
Mo-Zn/γ-Al_2O_3-15 wt% MgO	0.92	0.61	n.d.
Mo-Mn/γ-Al_2O_3-15 wt% MgO	0.12	0.55	0.08

n.d = not detected

The acidic properties of the prepared catalysts were investigated by NH_3-TPD analysis. The NH_3-TPD results are summerized in Table 6. The NH_3-TPD result of γ-Al_2O_3 shows acid sites of different strengths i.e. weak, medium and strong. However, the NH_3-TPD results of Mo/γ-Al_2O_3 and Mo/γAl_2O_3-15 wt% MgO catalysts show only acid sites of weak and medium strengths. This shows that the incorporation of Mo and MgO into the γ-Al_2O_3 affect the distribution of the acid sites on the surface of catalysts where the strong acid sites of the γ-Al_2O_3 have been eliminated.

Similarly, all bimetallic catalysts show weak and medium acid sites temperature ranges in the NH_3-TPD. The NH_3-TPD results further demonstrate that the total amount of NH_3 uptake is greater for Mo-Mn/γ-Al_2O_3-15 wt% MgO catalyst, showing that the number of acid sites increases on the surface of the catalyst. The different electron transfer ability, metal-metal (like Mo-Zn, Mo-Sn and Mo-Mn) and metal-support interaction lead to different uptake of NH_3 as explained in the TPR section.

Table 6. Density of acidic sites of the prepared catalysts.

Catalyst	Density of acidic sites (mmol/g)		
	Weak	Medium	Strong
Mo/γ-Al_2O_3	0.73	0.070	n.d.
Mo/γ-Al_2O_3-15 wt% MgO	0.95	0.038	n.d.
Mo-Sn/γ-Al_2O_3-15 wt% MgO	0.98	0.041	n.d.
Mo-Zn/γ-Al_2O_3-15 wt% MgO	1.21	0.081	n.d.
Mo-Mn/γ-Al_2O_3-15 wt% MgO	1.45	0.120	n.d.

n.d = not detected

3.2. Catalytic Activity of γ-Al_2O_3-15 wt% MgO Supported Bimetallic Catalysts

The catalyst screening and catalytic activity of different Mo/γ-Al_2O_3-MgO with varying contents of MgO has been discussed in detail in our previous published paper[11]. The result showed that catalyst with 15 wt % MgO exhibited excellence catalytic performance and provided biodiesel yield of 85.1wt% under optimized reaction conditions of 100 ^oC reaction temperature, catalyst

loading of 5wt%, methanol to oil ratio of 27:1, reaction time of 4h and stirring speed of 500 rpm. Similarly, the biodiesel yield of 63.8wt% was noted for γ-Al_2O_3-15wt% MgO mixed oxide catalyst at optimized reaction conditions. This catalyst was further modified with different metal oxides of Mn, Zn and Sn to design an effective catalyst for biodiesel production from WCO. The catalytic activity of the γ-Al_2O_3-15 wt% MgO supported bimetallic catalysts was investigated in the production of biodiesel from WCO under optimized reaction conditions i.e. reaction temperature of 100 ^oC, reaction time of 240 min, catalyst loading of 5 wt% (based on the amount of oil), methanol to oil molar ratio of 27:1 and agitation speed of 500 rpm. The results show (Figure 5) that the catalytic performance of the Mo/γ-Al_2O_3-15 wt% MgO catalyst increases when a second metal (Sn, Zn or Mn) was introduced. However, among the different bimetallic catalysts tested, the Mo-Mn/γ-Al_2O_3-15 wt% MgO catalyst shows better catalytic activity and provides the highest biodiesel yield of 91.4% as compared to the Mo-Sn/γ-Al_2O_3-15 wt% MgO and Mo-Zn/γ-Al_2O_3-15 wt% MgO catalysts which provide maximum biodiesel yield of 87.1% and 89.5% respectively at the similar reaction conditions. This shows that the introduction of a second metal Sn, Zn or Mn further modifies the number of active sites on the surface of the Mo/γ-Al_2O_3-15 wt% MgO catalyst, thus makes the biodiesel production process more effective from the WCO [40].

The high catalytic activity of the Mo-Mn/γ-Al_2O_3-15 wt% MgO catalyst could be due to the availability of the optimum number of catalytic active sites on the surface of the catalyst for the simultaneous transesterification-esterification reaction in the WCO. As shown in the TPD results, Mn modified catalyst shows greater number of acid-base catalytically active sites of different strength as compared to Zn and Sn modified catalysts. This indicates that the co-existence of catalytically active sites of different strengths are sufficient to carry out

simultaneous transesterification-esterification reaction in the WCO, thereby show excellent catalytic activity in high biodiesel yield. The strongest base would not necessarily be the best catalyst for a given transesterification reaction. A solid heterogeneous catalyst with strong basic sites may hold up the product molecules strongly, therefore the products can not desorbs after the reaction. On the other hand, the reactants may not be attracted to adsorb on the surface of a solid base catalyst that is too weak, thus reaction could not be initiated. Therefore, an optimum strength of the basic active sites are required for a given reaction [41].

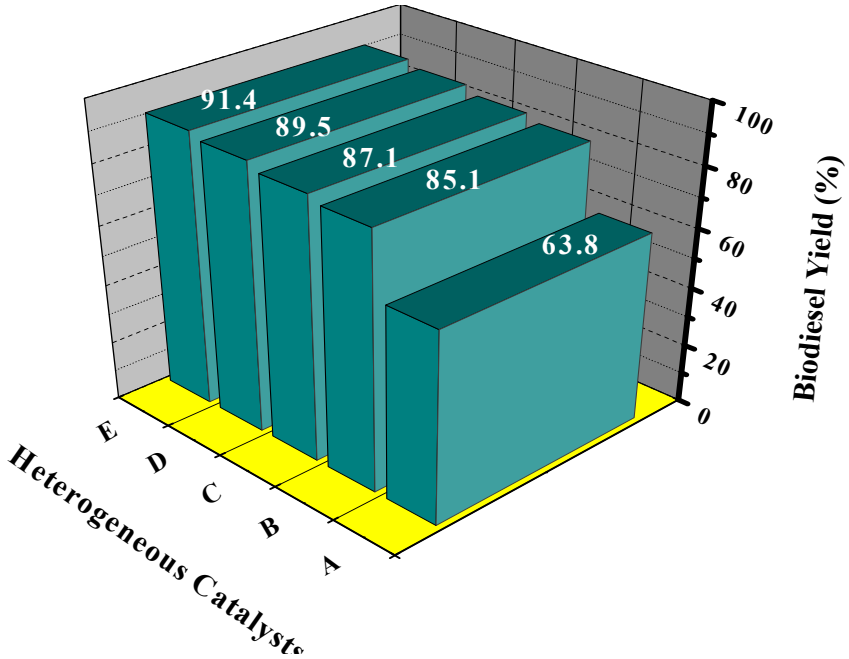

Figure 5. Catalytic activity of different heterogeneous catalysts at reaction time of 240 min, methanol/oil molar ratio of 27:1, catalyst loading of 5 wt%, reaction temperature of 100 ^{o}C and the agitation speed of 500 rpm.

Where

A; γ-Al_2O_3-15 wt% MgO, B; Mo/γ-Al_2O_3-15 wt% MgO, C; Mo-Sn/γ-Al_2O_3-15 wt% MgO, D; Mo-Zn/γ-Al_2O_3-15 wt% MgO, E; Mo-Mn/γ-Al_2O_3-15 wt% MgO.

3.3. Biodiesel quality evaluation

The properties of the biodiesel obtained from the WCO via simultaneous transesterification-esterification reactions were compared with the standard specifications of the American Standards for Testing and Materials (ASTM D-6751) and European Standards (EN 14214) (Table 7). It was noticed that the fuel properties of the prepared biodiesel are comparable to those reported in the literature and are within the limits imposed by the ASTM D-6751 and EN 14214 standard specifications. The major components of the synthesized biodiesel as identified by GC-MS analysis are methyl tetradecanoate (1.17%), methyl hexadecanoate (36.77%), methyl octadecanoate acid (27.70%), methyl 9-octadecenoate (19.21%), 9,12-octadecadienoate (11.60%).

Table. 7. Properties of synthesized biodiesel [42, 43]

Property	Unit	ASTM D-6751	EN 14214	Synthesized Biodiesel
Kinematic viscosity at 40 ºC	mm^2/s	1.9-6.0	3.50-5.00	4.02
Density (15 ºC)	kg/m^3	860-894	860-900	879
Flash point	^oC	>120	>120	175
Moisture content	%	< 0.05	< 0.05	0.01
Acid value	mg KOH/g	≤ 0.5	< 0.5	0.17
Methyl ester content	%	> 96.5	> 96.5	98.94
Cetane number	------	48-60	>51	57.8
Calorific value	J/g	------	------	40110
Monoglycerides	%mass	------	< 0.8	< 0.38
Diglycerides	%mass	------	< 0.2	< 0.082
Triglycerides	%mass	------	< 0.2	< 0.068
Glycerol	%mass	0.02	0.02	0.013

3.4. Kinetic approach

Transesterification reaction of the triglyceride with an alcohol in the presence of a suitable catalyst produces three molecules of alkyl esters and one molecule of glycerol as presented in Eq. 4.

$$Triglyceride + Alcohol \xrightarrow{Catalyst} 3\,Alkyl\ \ ester + Glycerol \qquad \text{[Eq. 4]}$$

Generally, transesterification reaction proceeds through three consecutive reversible reactions, where triglycerides are converted into diglycerides, monoglycerides and finally converted to glycerol (Eq. 5-7). During each step of the transesterification of glycerides, one molecule of ester is formed [44-46]. However, for convenience the intermediated reactions of diglyceride and monoglyceride are ignored and the three steps are combined in a single step as shown in (Eq. 4) [47, 48].

$$Triglyceride + ROH \xrightarrow{Catalyst} Diglyceride + RCOOR_1 \qquad \text{[Eq. 5]}$$

$$Diglyceride + ROH \xrightarrow{Catalyst} Monoglyceride + RCOOR_2 \qquad \text{[Eq. 6]}$$

$$Monoglyceride + ROH \xrightarrow{Catalyst} Glycerol + RCOOR_3 \qquad \text{[Eq. 7]}$$

Where R_1, R_2 and R_3 represents alkyl groups.

To study the kinetics of the transesterification reaction of the WCO, it is supposed that the transesterification reaction in the presence of Mo-Mn/Al_2O_3-15 wt% MgO as a bifunctional solid heterogeneous catalyst and methanol takes place in a single step, and that the catalyst amount is enough with respect to the oil to drive the reaction in the forward direction to form methyl esters. As a result, the reverse reaction and the change in the catalyst concentration during the course of

reaction are supposed to be negligible[49]. Therefore, the rate law for the forward transesterification reaction (ester formation) is expressed as follow [48, 50];

$$Rate = -r_A = \frac{-d[C_g]}{dt} = k^*[C_g].[ROH]^3 \qquad \text{[Eq. 8]}$$

Where [C_g] represents the concentration of the glycerides, [ROH] is the concentration of the alcohol and k^* is the equilibrium rate constant. Since methanol was used in the present work, therefore the above equation can be written as;

$$Rate = -r_A = \frac{-d[C_g]}{dt} = k^*[C_g].[CH_3OH]^3 \qquad \text{[Eq. 9]}$$

The overall reaction should follow a forth order reaction rate, however due to the use of an excess methanol, the concentration of the methanol is supposed to remain constant during the course of reaction. As a result, the reaction obeys the pseudo-first order kinetics [8, 49-51]. Thus, the rate expression can be written as;

$$Rate = -r_A = \frac{-d[C_g]}{dt} = k\ [C_g] \qquad \text{[Eq. 10]}$$

Or

$$Rate = -r_A = \frac{d[C_g]}{[C_g]} = -k\ dt \qquad \text{[Eq. 11]}$$

Where, k is the modified rate constant.

$$k = k^*[CH_3OH]^3$$

On integrating Eq. (11), we get

$$\ln[C_g] = -k\ t + c \qquad \text{[Eq. 12]}$$

Where, c is the integration constant. Let suppose that the initial concentration of the glyceride is [C_{g0}] at time t=0, then Eq. 12 becomes:

$$\ln[C_{g0}] = -k\ (0) + c \qquad \text{[Eq. 13]}$$

OR

$$\ln[C_{g0}] = c \qquad \text{[Eq. 13a]}$$

Substituting Eq. (13a) into Eq. (12) we get,

$$\ln[C_g] = -k\ t + \ln[C_{g0}] \qquad \text{[Eq. 14]}$$

Or

$$\ln[C_g] - \ln[C_{g0}] = -k\ t \qquad \text{[Eq. 14a]}$$

Or

$$\ln\frac{[C_g]}{[C_{g0}]} = -k\ t \qquad \text{[Eq. 14b]}$$

The fraction of the glyceride molecules that were converted to biodiesel esters (conversion of methyl ester was calculated by using the GC-FID:

$$X_{ME} = \frac{[C_{g0}] - [C_g]}{[C_{g0}]} = 1 - \frac{[C_g]}{[C_{g0}]} \qquad \text{[Eq. 15]}$$

Or

$$(X_{ME} - 1) = \frac{[C_g]}{[C_{g0}]} \qquad \text{[Eq. 15a]}$$

Where, X_{ME} represents the fractional conversion of the biodiesel esters.

Comparing Eq. (14b) and Eq. (15a), the result is

$$\ln(X_{ME} - 1) = -kt \qquad \text{[Eq. 16]}$$

Or

$$-\ln(1 - X_{ME}) = kt \qquad \text{[Eq. 16a]}$$

The $-\ln(1-X_{ME})$ was plotted versus reaction time at different reaction temperatures to determine the reaction order and the rate constants for the biodiesel production from the WCO in the presence of the Mo-Mn/Al_2O_3-15 wt% MgO as a bifunctional heterogeneous catalyst (Figure 6).

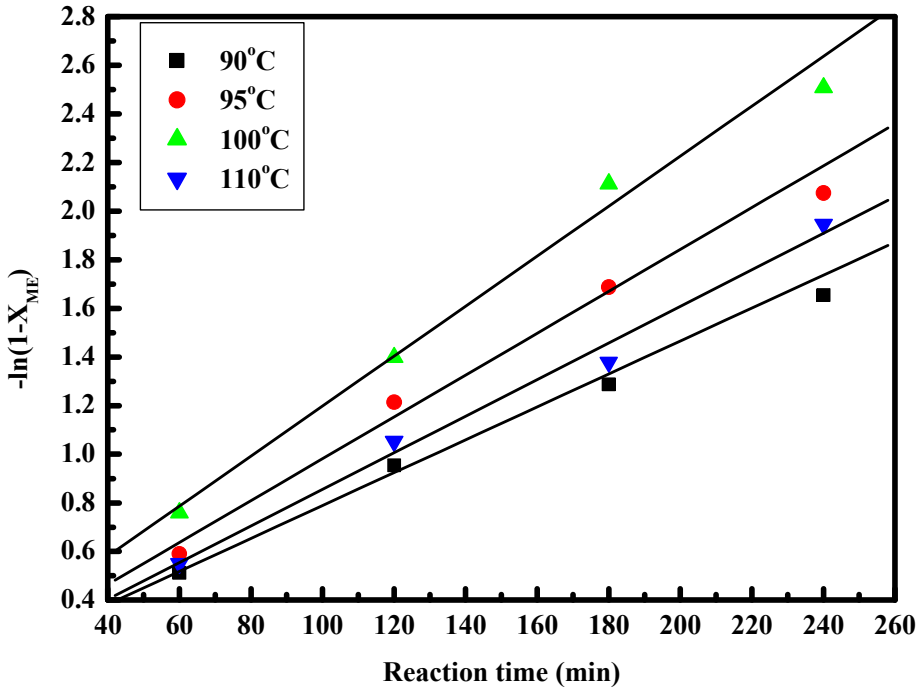

Figure 6. Plots of $-\ln(1-X_{ME})$ versus reaction time at different temperatures for the biodiesel production from the WCO in the presence of bifunctional Mo-Mn/Al_2O_3-15 wt% MgO catalyst

using the methanol to oil molar ratio of 27:1 and catalyst loading of 5 wt%.

All the plots between the $-\ln(1-X_{ME})$ verses time at different temperatures are linear, therefore supports the hypothesis that the reaction is of pseudo-first order.

The activation energy (*Ea*) was calculated by Svante Arrhenius equation, which gives the quantitative basis for the relationship between the activation energy, reaction rate constant and temperature as represented in Eq. 17.

$$k = Ae^{\frac{-Ea}{RT}} \qquad \text{[Eq. 17]}$$

Where k is the rate constant, representing the number of collisions among the reactants which result in a reaction (effective collisions), A is the pre-exponential factor or simply the pre-factor, represents the total number of collisions (leading to reaction or not), R is the universal gas constant and Ea is the activation energy, which is necessary for a chemical reaction to occur.

Taking integration of Eq. (17), we get,

$$\ln k = \ln A - \frac{Ea}{R} \cdot \frac{1}{T} \qquad \text{[Eq. 18]}$$

The activation energy (*Ea*) and the frequency factor (A) were calculated from the slope and intercept of the graph between the lnk versus 1/T x 10^3 as shown in Figure 7. The activation energy (*Ea*) was found to be 58.97 kJ/mol and the frequency factor (A) was calculated to be 1.88 x 10^6 min^{-1}. The reaction rate constant for the biodiesel production from the WCO in the presence of selected bifunctional heterogeneous catalyst and methanol was found to be 0.0104 min^{-1}.

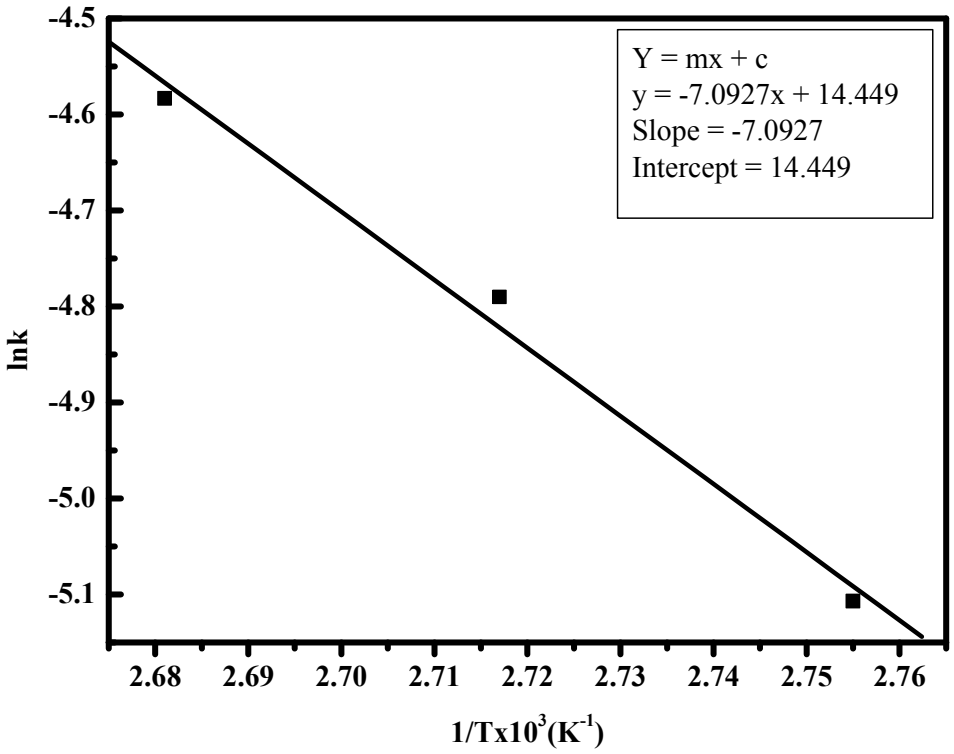

Figure 7. Arrhenius plot of lnk versus 1/T x 10^3 (K^{-1}) for biodiesel production from the WCO in the presence of Mo-Mn/γ-Al_2O_3-15 wt% MgO catalyst.

The activation energy for the biodiesel production from the WCO has good agreement with the literature and falls within the range of the activation energy obtained for the transesterification of soybean oil i.e. 33.6-84kJ/mol [48, 51].

Moreover, the kinetic studies suggest that the activation energy required for the simultaneous transesterification-esterification reactions in the selected WCO for the biodiesel production in the presence of Mo-Mn/Al_2O_3-15 wt% MgO bifunctional heterogeneous catalyst and methanol is reasonable, therefore can be a very useful to produce low cost biodiesel for the sustainable development and economic growth.

Thus, it can be said that the synthesized bifunctional heterogeneous solid catalyst has the

immense potential to be used in large scale biodiesel production from the low cost feedstocks such as waste cooking oil to replace the diesel fuel in the near future.

3.5. Catalyst reusability

The catalyst reusability is an important feature to minimize the cost of the overall biodiesel production process. A series of simultaneous transesterification-esterification experiments were performed under optimized reaction conditions to evaluate the catalytic activity of Mo-Mn/γ-Al2O3-15wt% MgO catalyst for sustainable biodiesel production from selected WCO. After each reaction, the recovered catalyst was first washed with methanol to remove the organic deposits (unreacted oil, biodiesel and glycerol), dried at 100 ^{o}C for 12 h, calcined at 500 ^{o}C for 2 h and later employed in the next experiment with new batch of WCO. The results for consecutive runs are shown in Table 8. The selected catalyst showed substantial reusability for at least 8 cycles without any deactivation under optimized reaction conditions. However, the biodiesel yield slowly decreases as the number of repeated use increases and the decrease became significant after eight times usage. The loss of the transesterification-esterification activity in the reusability tests could probably be attributed to the decrease in the active sites present on the surface of catalyst due to the deposition of the unwanted organic materials during the simultaneous transesterification-esterification reactions in the WCO [52, 53].

Table 8. Reusability Test

Number of run	Biodiesel Yield (%)
1st run	91.4
2nd run	90.9
3rd run	89.8
4th run	88.6
5th run	87.1
6th run	85.2
7th run	82.3
8th run	77.9
9th run	73.0
10th run	67.2

4. Conclusion

In the present study, bifunctional heterogeneous catalysts were successfully synthesized and employed in biodiesel production from WCO carrying simultaneous esterification of FFA and transesterification of triglycerides to develop an efficient and eco-friendly process for biodiesel production. Among different synthesized catalysts, Mo-Mn/γ-Al_2O_3-15wt%MgO catalyst showed excellent catalytic activity and provided maximum biodiesel yield of 91.4% under optimized reaction conditions as compared with Zn and Sn modified catalyst. The high catalytic activity of the Mn modified catalyst may be attributed to the co-existence of optimum number of acid-base sites on the surface of the catalyst. The kinetic studies further suggested that the biodiesel production from WCO in the presence of Mn modified bifunctional catalyst follows the pseudo-first order kinetics with activation energy (*Ea*) of 58.97 kJ/mol, frequency factor (A) 1.88 x 10^6 min^{-1} and the rate constant 0.0104 min^{-1}. It is observed that the activation energy required

for the simultaneous transesterification-esterification reactions in the selected WCO for biodiesel production is reasonable, therefore, the reaction is thermodynamically feasible.

Acknowledgements

The authors hereby acknowledge the University Technology PETRONAS, Malaysia for financial support to complete this project.

References

1. R. Raman, E. Panarella and C. National Research Council, Ottawa.
2. T. X. Liu and L. Kang, *Recent Advances in Entomological Research: From Molecular Biology to Pest Management*, Springer Berlin Heidelberg, 2011.
3. A. K. Agarwal, *Progress in Energy and Combustion Science*, 2007, **33**, 233-271.
4. M. R. Islam, A. B. Chhetri and M. M. Khan, *Greening of Petroleum Operations: The Science of Sustainable Energy Production*, Wiley, 2011.
5. A. Demirbas, *Energy Conversion and Management*, 2009, **50**, 14-34.
6. A. E. Atabani, A. S. Silitonga, I. A. Badruddin, T. M. I. Mahlia, H. H. Masjuki and S. Mekhilef, *Renewable and Sustainable Energy Reviews*, 2012, **16**, 2070-2093.
7. K. Nina, H. Miroslav, B. Igor and Š. Viera, *Journal of Biomedicine and Biotechnology*, 2011, **2011**.
8. A. K. Singh and S. D. Fernando, *Chemical Engineering & Technology*, 2007, **30**, 1716-1720.
9. G. Chen, R. Shan, S. Li and J. Shi, *Fuel*, 2015, **153**, 48-55.
10. A. K. Endalew, Y. Kiros and R. Zanzi, *Biomass and Bioenergy*, 2011, **35**, 3787-3809.
11. M. Farooq, A. Ramli and D. Subbarao, *Journal of Cleaner Production*, 2013, **59**, 131-

140.

12. H. V. Lee, J. C. Juan and Y. H. Taufiq-Yap, *Renewable Energy*, 2015, **74**, 124-132.

13. B. H. Diya'uddeen, A. R. Abdul Aziz, W. M. A. W. Daud and M. H. Chakrabarti, *Process Safety and Environmental Protection*, 2012, **90**, 164-179.

14. M. P. Dorado, F. Cruz, J. M. Palomar and F. J. López, *Renewable Energy*, 2006, **31**, 1231-1237.

15. K. T. Tan, K. T. Lee and A. R. Mohamed, *Energy*, 2011, **36**, 2085-2088.

16. A. Pandey, C. Larroche, S. C. Ricke, C. G. Dussap and E. Gnansounou, *Biofuels: Alternative Feedstocks and Conversion Processes*, Elsevier Science, 2011.

17. M. Farooq, A. Ramli and D. Subbarao, *Journal of Chemical & Engineering Data*, 2012, **57**, 26-32.

18. M. Tariq, S. Ali, F. Ahmad, M. Ahmad, M. Zafar, N. Khalid and M. A. Khan, *Fuel Processing Technology*, 2011, **92**, 336-341.

19. BSI, 2003, 1-19.

20. EN14105:2003, 1-19.

21. Q. Yu, X. Wu, C. Tang, L. Qi, B. Liu, F. Gao, K. Sun, L. Dong and Y. Chen, *Journal of Colloid and Interface Science*, 2011, **354**, 341-352.

22. R. B. Duarte, S. Damyanova, D. C. de Oliveira, C. M. P. Marques and J. M. C. Bueno, *Applied Catalysis A: General*, 2011, **399**, 134-145.

23. T. Borowiecki, W. Gac and A. Denis, *Applied Catalysis A: General*, 2004, **270**, 27-36.

24. X. Li, W. Zhang, S. Liu, L. Xu, X. Han and X. Bao, *Journal of Catalysis*, 2007, **250**, 55-66.

25. L. Qu, W. Zhang, P. J. Kooyman and R. Prins, *Journal of Catalysis*, 2003, **215**, 7-13.

26. Y. Zhang, Y. Zhou, L. Wan, M. Xue, Y. Duan and X. Liu, *Fuel Processing Technology*, 2011, **92**, 1632-1638.

27. S. Rajagopal, H. J. Marini, J. A. Marzari and R. Miranda, *Journal of Catalysis*, 1994, **147**, 417-428.

28. P. Arnoldy, J. C. M. De Jonge and J. A. Moulijn, *The Journal of Physical Chemistry*, 1985, **89**, 4517-4526.

29. D. L. Hoang, S. A. F. Farrage, J. Radnik, M. M. Pohl, M. Schneider, H. Lieske and A. Martin, *Applied Catalysis A: General*, 2007, **333**, 67-77.

30. S. Galvagno, C. Crisafulli, R. Maggiore, A. Giannetto and J. Schwank, *Journal of thermal analysis*, 1987, **32**, 471-483.

31. Y. Zhang, Y. Zhou, J. Shi, X. Sheng, Y. Duan, S. Zhou and Z. Zhang, *Fuel Processing Technology*, 2012, **96**, 220-227.

32. Q. Tang, X. Huang, C. Wu, P. Zhao, Y. Chen and Y. Yang, *Journal of Molecular Catalysis A: Chemical*, 2009, **306**, 48-53.

33. Y. Qian, S. Liang, T. Wang, Z. Wang, W. Xie and X. Xu, *Catalysis Communications*, 2011, **12**, 851-853.

34. K. Miyoshi and Y. W. Chung, *Surface diagnostics in tribology: Fundamental principles and applications*, World Scientific, 1993.

35. M. F. Gomez, L. E. Cadús and M. C. Abello, *Solid State Ionics*, 1997, **98**, 245-249.

36. H. Wang, H. Guan, L. Duan and Y. Xie, *Catalysis Communications*, 2006, **7**, 802-806.

37. M. Kumar, F. Aberuagba, J. K. Gupta, K. S. Rawat, L. D. Sharma and G. Murali Dhar, *Journal of Molecular Catalysis A: Chemical*, 2004, **213**, 217-223.

38. W. Gac, *Applied Surface Science*, 2011, **257**, 2875-2880.

39. M. Bolognini, F. Cavani, D. Scagliarini, C. Flego, C. Perego and M. Saba, *Catalysis Today*, 2002, **75**, 103-111.

40. W. Jiang, H.-f. Lu, T. Qi, S.-l. Yan and B. Liang, *Biotechnology Advances*, 2010, **28**, 620-627.

41. D. C. Kannan, 2009.

42. J. M. Encinar, N. Sánchez, G. Martínez and L. García, *Bioresource Technology*, 2011, **102**, 10907-10914.

43. J. A. Melero, G. Vicente, G. Morales, M. Paniagua and J. Bustamante, *Fuel*, 2010, **89**, 2011-2018.

44. A. Demirbas, *Energy Conversion and Management*, 2008, **49**, 125-130.

45. M. J. Ramos, C. M. Fernández, A. Casas, L. Rodríguez and Á. Pérez, *Bioresource Technology*, 2009, **100**, 261-268.

46. F. Ataya, M. A. Dubé and M. Ternan, *Energy & Fuels*, 2007, **22**, 679-685.

47. D. Kusdiana and S. Saka, *Fuel*, 2001, **80**, 693-698.

48. A. Birla, B. Singh, S. N. Upadhyay and Y. C. Sharma, *Bioresource Technology*, 2012, **106**, 95-100.

49. L. Zhang, B. Sheng, Z. Xin, Q. Liu and S. Sun, *Bioresource Technology*, 2010, **101**, 8144-8150.

50. D. Vujicic, D. Comic, A. Zarubica, R. Micic and G. Boskovic, *Fuel*, 2010, **89**, 2054-2061.

51. B. Freedman, R. Butterfield and E. Pryde, *Journal of the American Oil Chemists' Society*, 1986, **63**, 1375-1380.

52. C. Ngamcharussrivichai, P. Totarat and K. Bunyakiat, *Applied Catalysis A: General*,

2008, **341**, 77-85.

53. Y. H. Taufiq-Yap, H. V. Lee, M. Z. Hussein and R. Yunus, *Biomass and Bioenergy*, 2011, **35**, 827-834.